Mott Gap Filling by Doping Electrons through Depositing One Sub-Monolayer Thin Film of Rb on $Ca_2CuO_2Cl_2$

Han Li(李寒), Zhaohui Wang(王朝晖), Shengtai Fan(范圣泰), Huazhou Li(李华州), Huan Yang(杨欢)*, and Haihu Wen(闻海虎)*

National Laboratory of Solid State Microstructures and Department of Physics, Collaborative Innovation Center of Advanced Microstructures, Nanjing University, Nanjing 210093, China

(Received 26 February 2024; accepted manuscript online 8 April 2024)

Understanding the doping evolution from a Mott insulator to a superconductor probably holds the key to resolve the mystery of unconventional superconductivity in copper oxides. To elucidate the evolution of the electronic state starting from the Mott insulator, we dose the surface of the parent phase $Ca_2CuO_2Cl_2$ by depositing Rb atoms, which are supposed to donate electrons to the CuO_2 planes underneath. We successfully achieved the Rb sub-monolayer thin films in forming the square lattice. The scanning tunneling microscopy or spectroscopy measurements on the surface show that the Fermi energy is pinned within the Mott gap but close to the edge of the charge transfer band. In addition, an in-gap state appears at the bottom of the upper Hubbard band (UHB), and the Mott gap will be significantly diminished. Combined with the Cl defect and the Rb adatom/cluster results, the electron doping is likely to increase the spectra weight of the UHB for the double occupancy. Our results provide information to understand the electron doping to the parent compound of cuprates.

DOI: 10.1088/0256-307X/41/5/057402

High-temperature superconductivity (HTSC) has continued to be the focus of studies in modern condensed matter physics since the discovery of cuprates. Despite significant efforts from both theoretical and experimental aspects, the mechanism of HTSC remains ambiguous. The band is half-filled in the parent compound of cuprates, however, the parent compound is a Mott insulator instead of the metal because of the strong correlation effect.[1,2] The physics can be appropriately described by the half-filled Hubbard model,[3,4] in which a strong local Coulomb interaction U prevents electrons from doubly occupying any single Cu $d_{x^2-y^2}$ orbital, resulting in the splitting of electronic states near Fermi energy into the so-called upper (UHB) and lower (LHB) Hubbard bands,[5] see Fig. 1(a). If the problem is further considered in the strong-coupling limit by the t–J model,[6] the low-energy electronic excitations of the charge transfer band (CTB) are predicted due to the planar σ hybridization of the Cu $d_{x^2-y^2}$ orbital with O $2p_{x,y}$ orbitals.[7] Then the energy gap of the parent compound is the charge transfer energy difference Δ_{Mott} instead of the strong on-site Coulomb interaction U.[8] In addition, based on this paradigm, a robust long-range antiferromagnetic (AF) order is stabilized in the Cu lattice coexisting with the intriguing electronic physics in the parent compound of cuprates.[9]

In cuprates, HTSC emerges by the chemical doping to the parent compound of the Mott insulator. Besides the pseudogap phase[10] or novel orders that compete or coexist with superconductivity,[2,11,12] the charge transfer physics of doped Mott insulators may be another key point for unraveling HTSCs. In the parent compound, when the CuO_2 planes are doped with charge carriers, the AF phase is suppressed together with the Mott gap filling and the appearance of the quasiparticle-like density of states (DOS) near the Fermi level. One compelling explanation is that the chemical potential shifts towards the CTB (or the UHB) to accommodate the doped holes (or electrons). Meanwhile, the many-body effect causes a transfer of the DOS from the UHB or CTB to fill in the Mott gap.[13,14] The doping evolution of the electronic structure in cuprates has been studied in various systems.[1,15–19] One must consider how the doped charge carriers destroy the Mott state and how the initial pairing is formed to generate superconducting gaps.[20] Our recent work is concerned with this issue, revealing the emergence of the low-energy gap in extremely hole underdoped cuprate superconductors.[21]

CCOC is a canonical half-filling AF Mott insulator, and there is a single CuO_2 plane in one structural unit cell. The substitution of a monovalent Na^+ for divalent Ca^{2+} results in hole doping of $Ca_{2-x}Na_xCuO_2Cl_2$ (Na-CCOC), and the maximum critical temperature is about 28 K.[22] A checkerboard electronic crystal state is observed in Na-CCOC,[23,24] and then it can be explained by nodal quasiparticles and antinodal charge ordering in this system.[25] These results are helpful for understanding the HTSC in cuprates. Moreover, electron doping has been achieved by utilizing surface deposition of alkali atoms on its double-layer sibling system $Ca_3Cu_2O_4Cl_2$.[26]

In this Letter, we report the studies on the electronic

*Corresponding authors. Email: huanyang@nju.edu.cn; hhwen@nju.edu.cn
© 2024 Chinese Physical Society and IOP Publishing Ltd

structure evolution of the CCOC system by dosing electrons through depositing Rb on the surface of the single crystal. We investigate the effect of the isolated Rb adatom/cluster as well as the Rb sub-monolayer film with ordered lattice at 78 K by scanning tunneling microscopy or spectroscopy (STM/STS). At the Rb adatom/cluster, the DOS of the UHB is enhanced while some in-gap states appear near the foot of the UHB. On the Rb lattice, the in-gap states are significantly enhanced and the Mott gap is reduced. Our findings reveal how the Mott gap is filled due to increasing electron concentration, which helps to understand the strong correlation effect of the parent phase with Mott insulating behavior.

Single crystals of CCOC were grown by the flux method.[27] The powder mixture of CaO and $CuCl_2$ with a 2:1 molar ratio was put into an alumina crucible. Then the crucible was heated to 780 ℃ and held at this temperature for 24 h to get the CCOC polycrystal. After an intermediate grinding, the precursor was heated to 780 ℃ and held for 5 h, then heated to 930 ℃ and held for 10 h. The ramp rate of temperature during the heating processes was 1 ℃/min. Finally, the melt was slowly cooled to room temperature at a rate of 1 ℃/min. High-quality single crystals were found with the size of millimeters. Single crystals were cleaved *in situ* at room temperature in ultrahigh-vacuum conditions up to 1.9×10^{-10} torr. The dosing of Rb atoms and STM/STS are performed with a cryogenic variable temperature ultrahigh vacuum STM (USM-1300, Unisoku Co., Ltd.). The Rb adatom/cluster or film growth was also carried out on the cleaved surface of CCOC. The Rb source (SAES group) was heated to about 600 ℃ (or 640 ℃), and the growth time for the Rb flux was several seconds (or about 1 min) to get the Rb adatoms/clusters (or the Rb film). After the deposition, the sample was immediately put back into the STM head through transferring in the ultra high vacuum atmosphere, which was kept at a low temperature of about 78 K. The electrochemically etched tungsten tip was used in this study, and the calibration was carried out on the single crystalline Au (111) surface. The tunneling spectra were recorded by using a standard lock-in amplifier technique with an AC oscillation of 25 mV (root-mean-square amplitude) and 973 Hz. All the tunneling data were taken at a temperature of about 78 K. We have tried the STM/STS measurements at liquid ^{4}He temperature, but it failed because of the huge tip-sample resistivity due to the highly insulating behavior of the CCOC samples.

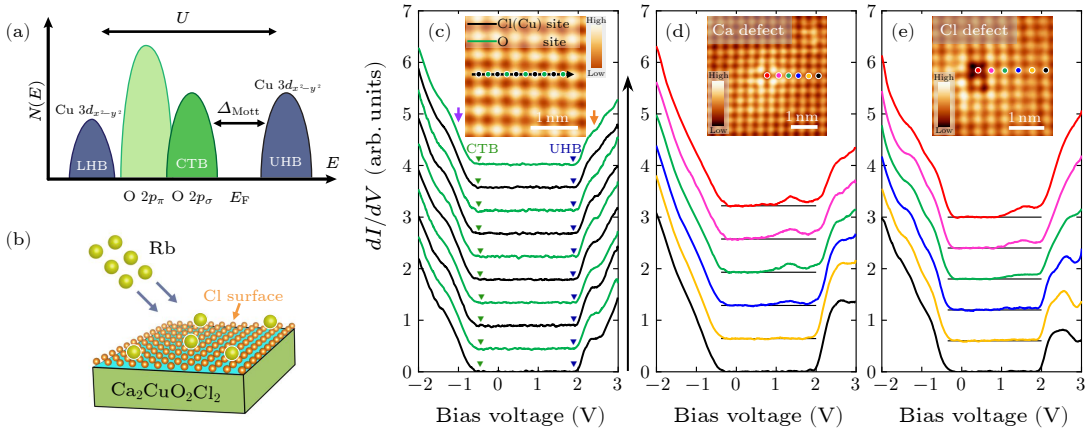

Fig. 1. (a) Schematic band structure of the parent Mott insulating phase of cuprates. (b) Schematic illustration of *in situ* Rb dosing onto CCOC surface. Electrons are introduced into the sample surface due to the physical absorption of Rb atoms. (c) Spatially resolved tunneling spectra measured along an arrow in the topography of CCOC shown as the inset ($V_{\rm set} = -2.5$ V, $I_{\rm set} = 100$ pA). The spectra in black are measured on Cl atoms on the surface or Cu atoms underneath, while the spectra in green are measured in the middle between two neighboring Cl atoms. Triangles in green mark tops of CTB, and those in blue mark bottoms of UHB. Purple and orange arrows roughly indicate the peak positions of CTB and UHB, respectively. (d) A series of tunneling spectra taken at and away from a Ca defect ($V_{\rm set} = -2.5$ V, $I_{\rm set} = 100$ pA). (e) A series of tunneling spectra taken at and away from a Cl defect ($V_{\rm set} = -2.0$ V, $I_{\rm set} = 100$ pA). Tunneling spectra in all panels are shifted for clarity. Each spectrum in (d) and (e) is plotted using the same color as the point marking the measured position.

In the crystal structure of CCOC, there is a single CuO_2 plane in one structural unit cell, and the CuO_2 planes are sandwiched by insulating CaCl layers. Therefore, the single crystal can be easily cleaved between the adjacent CaCl layers to expose a clean and atomically flat CaCl surface with an undistorted tetragonal crystal structure. Meanwhile, Cu atoms are directly underneath the Cl atoms on the exposed surface with a distance of about 2.75 Å. The undoped CCOC is a canonical Mott insulator, and a typical band structure of the Mott insulator is shown in Fig. 1(a). For CCOC, the charge transfer gap $\Delta_{\rm Mott}$ is about 2.1–2.2 eV from previous reports.[28,29] On the atomically flat Cl surface, we can deposit Rb atoms, see Fig. 1(b). The Rb adatom/cluster or the Rb sub-monolayer grown on the surface can introduce extra electrons to the sample, which may diminish the Mott gap of the sample.

Before the Rb deposition, we characterize the CCOC

substrate by doing the topographic image and tunneling spectrum measurement. An example is shown in Fig. 1(c). The inset in Fig. 1(c) shows the atomically resolved surface measured on CCOC sample, and one can see a perfect square lattice of Cl atoms with the lattice constant a_0 of about 3.86 Å. Here, the Cu atoms in the CuO_2 plane are just below the Cl atoms on the surface, while the O atoms are below the center between the two nearest neighboring Cl atoms. Tunneling spectra are measured along the Cl–Cl (or the Cu–O–Cu chain) direction, and they are shown in Fig. 1(c). Since the CaCl layers are insulating, the differential conductance dI/dV, which is related to the local density of states (DOS), should be dominated by electronic structure in the CuO_2 plane. The spectra in Fig. 1(c) show spatial homogeneity in the present scale at and between Cl sites, and there is a large gap across the Fermi energy. Features on the spectra can be understood by the schematic band structure of the Mott insulator shown in Fig. 1(a). The endpoints of the gapped feature at negative [marked by green triangles in Fig. 1(c)] and positive [marked by blue triangles in Fig. 1(c)] energy sides correspond to the top edge of the CTB and the bottom edge of the UHB, respectively.

Then the charge transfer gap Δ_{Mott}, defined as the energy difference between CTB and UHB, is about 2.3 eV from our data. This value is close to those reported previously by the optical reflectivity [28] and STS [29] measurements. In addition, the energy of the top edge of CTB is about −0.4 eV which is also similar to the values obtained by ARPES measurements. [30,31] Beyond the edges of the charge transfer gap, there are shoulders on the spectra at about −1.0 and 2.5 eV and they are indicated by purple and orange arrows in Fig. 1(c). It should be noted that these shoulders can exhibit as peaks on some spectra, and examples can be seen in Figs. 1(d) and 1(e). These shoulders or peaks of local DOS at negative and positive energies may correspond to peak positions of the CTB [32] and UHB, [29] respectively. The intense DOS appearing below −1.5 eV may originate from the O $2p_\pi$ band. [32]

Besides the perfect Cl lattice on the surface of CCOC, we observe two types of defects: one is the Ca vacancy [Fig. 1(d)], and the other is the Cl vacancy [Fig. 1(e)]. A Ca defect may result in the atomic relaxation of the four nearest Cl atoms on the surface and make them higher. [33] Here, a Ca vacancy is equivalent to doping two holes to the CuO_2 plane, while a Cl vacancy donates an electron. These defects provide natural platforms for studying the Mott gap filling to the parent compound, but the defect induced states are quite localized. From the tunneling spectra shown in Figs. 1(d) and 1(e), one can see that the spectra measured just above the Ca or Cl defects show similar behavior, i.e., a broad electronic state appears near the bottom edge of the UHB within the charge transfer gap. The in-gap states finally disappear on the spectrum measured $5a_0$ away from the vacancy sites. Based on the theoretical calculation, hole doping may induce the in-gap state near the CTB, [13] and the in-gap state may move to the UHB due to a repulsive impurity potential. [34] Meanwhile, electron doping can also induce an in-gap state below the UHB. [35] However, we would argue that the location of the local DOS peak induced by the Ca or Cl vacancies seems to be an effect strongly linked with the edge of the UHB, but not the repulsive impurity potential effect, since their locations and features look quite similar, despite the impurities of Cl and Ca vacancies are very different. Although the in-gap states in situations of both hole and electron doping sides are very similar, the influences on the DOS of the UHB by different kinds of doping are very different. One can see that at the Cl vacancy, the DOS shows an obvious enhancement above 2 eV, which is weaker for the Ca site. It should be noted that the measured dI/dV is related to but not simply equal to the local DOS because of the matrix element effect. Therefore, the enhancement of the spectrum weight of the UHB needs further careful investigation, but the in-gap state seems to be independent of the matrix element effect.

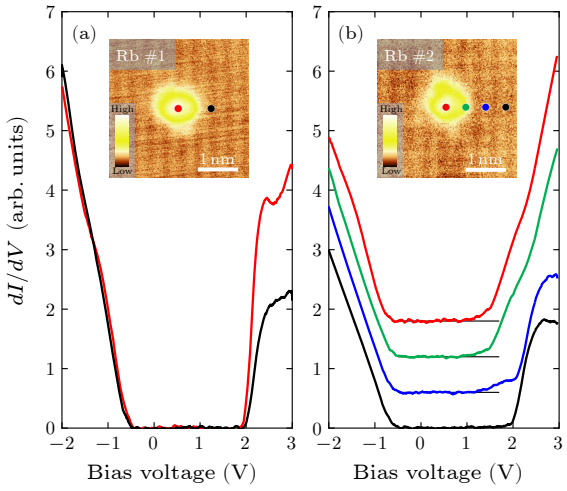

Fig. 2. (a) Tunneling spectra measured on and away from the Rb adatom or cluster 1 deposited on CCOC surface ($V_{\mathrm{set}} = -2.5$ V, $I_{\mathrm{set}} = 100$ pA). (b) Tunneling spectra measured at different sites across the Rb atom or cluster 2 ($V_{\mathrm{set}} = -2.5$ V, $I_{\mathrm{set}} = 100$ pA). Each spectrum in this figure is plotted using the same color as the point marking the measured position. Tunneling spectra in (b) are shifted for clarity. The diameters of two adatoms or clusters are both about 1 nm, while the heights are about 0.13 and 0.10 nm for clusters 1 and 2, respectively. However, these two adatoms or clusters have significantly distinct alterations to the background electronic structures.

In order to investigate the doping effect with a higher doping level than a Cl vacancy, we deposit Rb atoms to the top Cl surface of CCOC. When the depositing time is short, isolated Rb adatoms or clusters can be observed on the top surface of the Cl lattice. Insets in Fig. 2 show topographic images of the Rb adatom or the Rb cluster on the surface, and their diameters are both about 1 nm while their heights are about 0.13 and 0.10 nm for clusters 1 and 2, respectively. From the spectra shown in Fig. 2(a), we cannot see the peak of local in-gap DOS as formed for the Cl vacancies, which may be induced by the lower electron doping level by the Rb adatom/cluster 1 than that by the Cl vacancy. The obvious effect of the Rb atom is the significant enhancement of the DOS of the UHB, but

the in-gap states cannot be seen within the charge transfer gap on the spectra. For the Rb adatom/cluster 2, the electron doping level seems to be higher than the Cl vacancy. The spectrum measured about 1 nm away from the adatom/cluster as plotted in blue is similar to that measured just on the Cl vacancy. When the tip moves to the positions just above the Rb adatom/cluster 2, the spectral weight of the UHB is significantly enhanced. The in-gap states are also enhanced near the edge of the UHB leading to a general elevating of the DOS smoothly connected to the enhanced DOS of the UHB, meanwhile the Mott gap has also been significantly suppressed, i.e., it changes from about 2.35 to about 1.6 eV. Clusters 1 and 2 are two representative examples of two kinds of Rb adatoms/clusters we found. The clusters like 2 show a clear Mott-gap filling effect, while those like 1 have little influence on the gap filling. Usually, clusters like 2 are slightly larger than those like 1, which suggests that there may be more Rb atoms in clusters like 2 than those like 1. Therefore, the magnitude of charge transfer should be greater for clusters like 2. The other possibility is that adatoms/clusters like 2 are closer to the substrate because of the lower height, thus they can lose electrons more easily than the case of cluster 1. The above-mentioned reasons may result in the different amounts of the charge transfer to the CuO_2 plane from adatoms/clusters like 2 or those like 1 and therefore induce the spectral differences between clusters 1 and 2. With the increase of the electronic doping level, the effective doping influenced range of the Rb adatom/cluster for cluster 2 becomes larger than for cluster 1. With longer depositing time, Rb atoms form an ordered lattice on the CCOC surface instead of the isolated Rb adatoms/clusters. The inset in Fig. 3(a) shows a topographic image of a Rb film with an areal density of about 0.012 Rb/Cl (or Rb/Cu). This is a rectangular lattice with lattice constants of about 35 and 38 Å with a small anisotropy of about 1.08. The dosed atoms of alkali metal usually have a very disordered distribution[36,37] or form some locally ordered lattice[38–40] on different substrates, as far as we know, the ordered lattice in a very large scale has not been observed before. The Rb lattice may be hexagonal without Rb-substrate interaction, and the hexagonal lattice does appear when it is grown on another substrate.[37] Therefore, the CCOC substrate plays an important role in the formation of the square lattice by Rb atoms.

Since we have successfully grown the Rb film with a regular lattice on CCOC, it is very interesting to investigate the electronic properties of the sample. Here it should be noted that the Rb atoms are grown on the Mott insulator of CCOC, and the valence electrons of Rb atoms are supposed to go to the CuO_2 plane, leaving only Rb^+ ions on the top layer. The Cl ions on the top surface of the substrate form a perfect structure with one block unit layer of the copper oxide octahedra containing a single CuO_2 plane, thus they should have closed shells of electrons and are insulating. In this point of view, the measurements on the lattice of Rb ions on the surface can reflect the Mott insulating nature of the CuO_2 plane of the substrate of CCOC. Strikingly, here the size of the Rb ion determined from the topography seems to be quite large, i.e., the effective diameter of a Rb ion seems to be close to the lattice constant of (3.6 nm on average). This is certainly not the real size, but showing an extended influence of DOS affected by the Rb ions. Then we measure the tunneling spectra at the Rb centers, in the middles of the two nearest neighbored Rb ions, and at the centers of a rectangle block of four Rb ions, and we plot the averaged spectra measured at these three positions in Fig. 3(a). One can see that the spectra almost overlap with each other except for the part in the high energy region for the UHB. The DOS is slightly enhanced above 2 eV at the Rb site, which may suggest a slightly higher electron doping level at the center of the Rb ion. However, the in-gap states have very little energy dependence at different positions. In some places, we can see Rb vacancies, and one example is shown in the inset of Fig. 3(b). However, based on the spectra shown in Fig. 3(b), the Rb vacancy has negligible influence on the spectrum. In other words, the neighboring Rb ions to the vacancy have an influential range of about 3.6 nm which is much larger than that of $3a_0 \approx 1.2$ nm estimated for the Ca or Cl vacancies, as shown in Fig. 1. Meanwhile, it should be considered that the Rb vacancy is surrounded by Rb ions, as we argued above, this will give rise to extended DOS to the vacancy site. The overlapping influences of all neighboring Rb irons may fill the Rb vacancy's influence on the in-gap state.

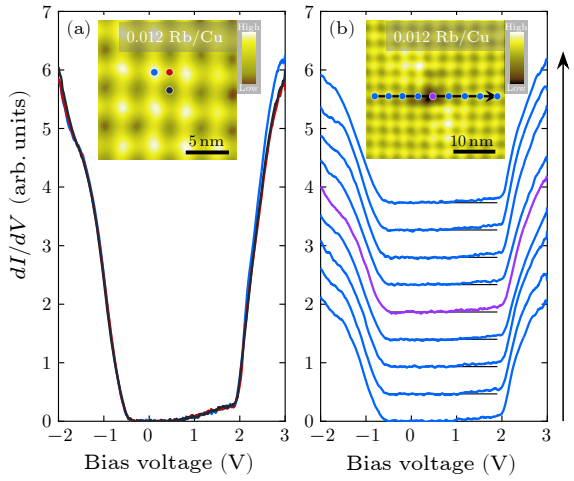

Fig. 3. (a) Averaged tunneling spectra measured at different sites on the Rb film grown on the CCOC surface with the areal density of about 0.012 Rb/Cu. The topographic image of the Rb film is shown in the inset. The typical sites are marked by colored points in the inset, and each spectrum in the main panel is plotted using the same color as the point. (b) Tunneling spectra measured across a Rb defect in the Rb film ($V_{set} = -2.5$ V, $I_{set} = 100$ pA). Spectra are shifted for clarity in this figure. Spectra show spatial uniformity when across the defect.

In the Rb sub-monolayer grown on the CCOC substrate, the electron states are almost homogeneous in nanoscale. With the increase of the deposition time, the Rb sub-monolayer with different areal densities can be obtained. Figures 4(a) and 4(b) display two examples of the Rb sub-monolayer with different lattice constants. The lat-

tice shown in Fig. 4(a) is the same as those shown in Fig. 3, and the areal density is about 0.012 Rb/Cu. The rectangular lattice has the lattice constants of 3.8 and 3.5 nm. Figure 4(b) shows the topography of a Rb sub-monolayer with an areal density of about 0.017 Rb/Cu, and the lattice now becomes almost a square shape with a lattice constant of about 2.9 nm. The change from the rectangular lattice to the standard square lattice may be induced by a larger areal density of Rb resulting in a stronger repulsive interaction between two neighbored Rb ions. Figure 4(c) shows the averaged tunneling spectra measured on different Rb sub-monolayers. One can see that with the increase of the areal density of Rb, the in-gap states are significantly enhanced and then overlapped with the UHB [Fig. 4(d)], resulting in a clear suppression of the Mott gap. We note that the dI/dV value at about -1 V seems to downshift slightly with increasing Rb coverage in Fig. 4(c). However, as mentioned above, the measured dI/dV is related to but not simply equal to the local DOS due to the matrix element effect, and there is the normalization effect due to the setpoint condition in the spectrum measurement. Therefore, it is difficult to know how the DOS changes in the CTB with the variation of the doping level. It should be noted that starting energy of the edges of the CTB at about -0.5 eV does not have obvious shifts for different spectra shown in Fig. 4(c), which is different from the picture with a chemical potential shift or jump observed in other p- and n-type cuprates.[26,41–43]

From our results, a striking observation is that the chemical potential of Cl-vacancy, Ca-vacancy, Rb adatoms or clusters and Rb films all stays fixed in the charge transfer gap but is closer to the CTB, which echoes with the pinned chemical potential at low doping.[44,45] However, the fixed chemical potential in the charge transfer gap among Ca and Cl vacancies is contrast to the expectation of the anomalous spectral-weight transfer picture for a doped Mott system.[13] In addition, the sub-monolayer films and different vacancies cause a very similar in-gap state, although they are expected to hole-dope for the Ca vacancy and electron-dope for others. One may not expect the appearance of in-gap state near the bottom of the UHB for hole-dope case. As a matter of fact, the feature of the unconventional in-gap state induced by Ca vacancy is quite similar with the previous report.[46] We note that there is a theoretical calculation concerning repulsive impurity potential that try to explain this unconventional in-gap state.[34] However, to unravel the origin of the Ca vacancy induced in-gap state may require further theoretical studies.

In the presence of a Rb adatom/cluster or the Rb sub-monolayer, the effective range for a single adatom/iron is about 1.2–1.5 nm, which is much larger than the Cu–Cu distance a_0 in the CuO_2 layer. This may suggest a partial delocalization effect because the doped electron is supposed to go to the Cu site beneath forming a doublon of two electrons. In fact, the localization effect of the electron doublon depends on the magnetic structure of the background. For instance, in a paramagnetic environment, the doublon is supposed to be completely delocalized and can form a band. In this work, we observe an effective range of about $3a_0$ for the doped electrons and there are no metallic states formed at the Fermi level, which suggests that the double occupancy state seems only partially delocalized.[47] It should be noted that the background is a Mott insulator with the antiferromagnetic order, and the charge transfer happens between the Rb atoms on the surface and the Cu sites underneath the surface CaCl layer. These reasons may induce the partial delocalization of the doublon. In addition, other reasons such as structural deformations or phonons possibly due to the Rb atoms may also lead to the experimental observation. However, to unravel the origin of this effect requires further theoretical studies.

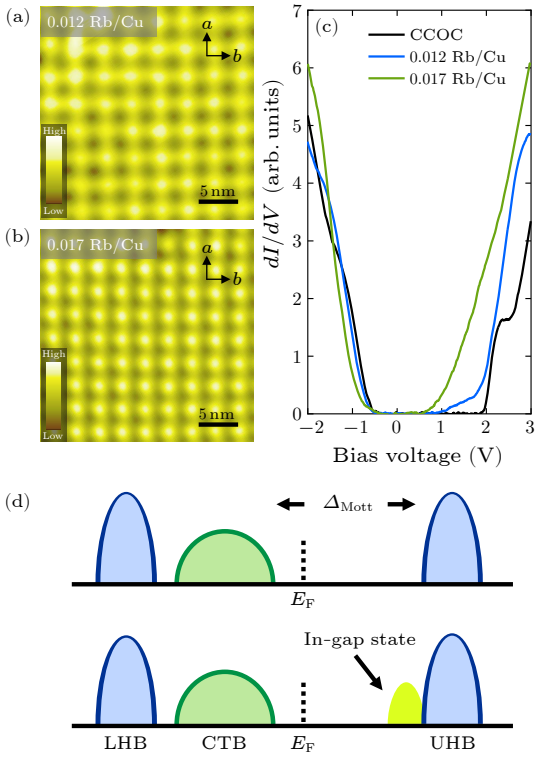

Fig. 4. Topographic image of Rb films grown on the CCOC surface with the areal density of (a) about 0.012 Rb/Cu and (b) about 0.017 Rb/Cu ($V_{set} = -2.5$ V, $I_{set} = 100$ pA). (c) Averaged tunneling spectra measured on CCOC and Rb films with different areal densities ($V_{set} = -2.5$ V, $I_{set} = 100$ pA). (d) Schematic drawing of the appearance of the in-gap states at the bottom of the UHB induced by Rb adatoms or Rb sub-monolayers. Here, E_F does not change.

The extraordinary large lattice constant of Rb films have never been found on cuprate systems before. The lattice constant in a and b directions for 0.012 Rb/Cu film are $\sim$10 and $\sim$9 times the lattice constants of CCOC, and both $\sim$7.6 times for 0.017 Rb/Cu film. The radii of the isolated Rb atoms and corresponding ion are 2.48 Å and 1.52 Å, respectively.[48] The spatial scales of Rb ions for 0.012 and 0.017 Rb/Cu film defined by full width at half maximum are $\sim$21 Å and $\sim$17 Å, respectively. It is $\sim$14 times the diameter of Rb cation for 0.012 Rb/Cu film and $\sim$11 times for 0.017 Rb/Cu film. As mentioned be-

fore, this size is certainly much larger than the real size of an individual atom or ion of Rb in vacuum, which is supposed to be induced by extended DOS of the Rb ion on the background of CCOC. We propose a scenario to comprehend the uniform electronic structure throughout the Rb lattice with extraordinarily large radii of Rb ions. When the density of adsorbed Rb atoms is beyond a certain threshold, a two-dimensional Rb film with a regular lattice is formed. The donated electron by a Rb atom will be absorbed by one Cu^{2+} to form a double occupancy state, which may locally enhance the hopping but weaken the correlation effect. This picture implies that the doped electrons donated by Rb atoms would dilute the spin system by neutralizing the spin on a 3 d^9 Cu site and adjust the spectral function[1] as well as super-exchange energy J,[3] forming a circular hopping active puddle centered on the Rb donor atom. For a single Rb atom on the CCOC background, this effect extends to a large distance compared with of the radii of a Rb individual atom or ion, but with a gradually decreased strength from the site of Rb to far away. Thus, the modified electronic wave function given by an individual Rb atom looks like a puddle. Each puddle contains one double occupancy state. When many Rb atoms form a reconstructed lattice, these puddles will overlap each other in the lattice. However, the state formed by the puddles is bounded by the Rb film area, and the motion of this double occupancy state is still prohibited by the correlation effect, resulting in a nontrivial insulating state.

The picture we proposed above can also explain why the measured size of each Rb atom looks so large, this is because the double occupancy state given by the donated electron of each Rb atom may be mobile to a certain distance which is much larger than the radii of the Rb atom itself. Several interesting properties remain to be explored to explain the large lattice constants, such as binding distance, charge transfer, and work function as adsorbed Rb atoms change from clusters to two-dimensional lattice. According to the anomalous spectral-weight transfer picture for doping electrons to the Mott insulator,[13] when one electron is doped to the system, both the LHB (or CTB) and the UHB will lose one electron state, but a new electron state with two electrons will appear at the lower edge of the UHB, and the Fermi energy will immediately jump from an in-gap energy to the lower edge of the UHB. However, our experiments [Fig. 4(d)] do not support this picture. Firstly, the Fermi energy seems to be pinned in the charge transfer gap. Secondly, some states start to accumulate in the charge transfer gap region near the edge of the UHB. Meanwhile, the DOS weight of the UHB gets enhanced, instead of weakened. One may argue that the enhancement of the spectrum weight of the UHB may be due to the matrix element effect. However, it should be noted that the spectrum shapes at negative energies are similar for spectra measured on CCOC and Rb sub-monolayers, and therefore the enhanced spectrum weight on the positive side is likely due to the chemical doping instead of the matrix element effect. In addition, the spectrum-weight enhancement of the UHB is also observed at Cl vacancy and the Rb adatom/cluster which also dope electrons to the CuO_2 plane. In contrast, the decrease of the spectrum weight is observed at the Ca vacancy with hole doping, which is consistent with a previous report.[46] Therefore, we conclude that the electron doping is likely to increase the spectra weight of the UHB for the double occupancy. We believe the electron doping will systematically change the spectral function and the super-exchange J values, thus leading to a complex modification of the whole electronic state. Our experiments expose distinctions from the anomalous spectral-weight transfer picture, which sheds new light on understanding the evolution of the doped Mott insulator, and intimately helps unraveling the mystery of the superconductivity mechanism in cuprates.

We have successfully grown thin films of Rb with periodic structures on a CCOC parent compound, which allows a detailed investigation on the doped Mott insulator of the parent phase of cuprate. The STM measurements of the Rb film reveal that the Fermi energy is close to the upper edge of the charge transfer band and is pinned within the Mott gap. We also find that the spectral weight of UHB is obviously enhanced by electrons from Rb donor atoms, in stark contrast to the expectation of the anomalous spectral-weight transfer picture which postulates that the weight of the UHB will be suppressed after doping electrons. Meanwhile, with increasing electron doping, broad in-gap states gradually set up near the bottom of UHB, and the Mott gap will be significantly diminished. The spectra measured on Rb thin films and Rb atoms or clusters show similar behavior. Our work provides a new clue to the understanding of Mott physics.

Acknowledgements. This work was supported by the National Natural Science Foundation of China (Grant Nos. 11974171, 12061131001, and 11927809) and the National Key R&D Program of China (Grant No. 2022YFA1403201).

References

[1] Lee P A, Nagaosa N, and Wen X G 2006 *Rev. Mod. Phys.* **78** 17
[2] Keimer B, Kivelson S A, Norman M R, Uchida S, and Zaanen J 2015 *Nature* **518** 179
[3] Anderson P W 1959 *Phys. Rev.* **115** 2
[4] Anderson P W 1987 *Science* **235** 1196
[5] Hirsch J E 1985 *Phys. Rev. B* **31** 4403
[6] Chao K A, Spałek J, and Oleś A M 1978 *Phys. Rev. B* **18** 3453
[7] Zaanen J, Sawatzky G A, and Allen J W 1985 *Phys. Rev. Lett.* **55** 418
[8] Emery V J 1987 *Phys. Rev. Lett.* **58** 2794
[9] Anderson P W 1950 *Phys. Rev.* **79** 350
[10] Alloul H, Rullier-Albenque F, Vignolle B, Colson D, and Forget A 2010 *Europhys. Lett.* **91** 37005
[11] Tranquada J M, Sternlieb B J, Axe J D, Nakamura Y, and Uchida S 1995 *Nature* **375** 561
[12] Ghiringhelli G, Le Tacon M, Minola M *et al.* 2012 *Science* **337** 821
[13] Eskes H, Meinders M B J, and Sawatzky G A 1991 *Phys. Rev. Lett.* **67** 1035
[14] van Veenendaal M A, Sawatzky G A, and Groen W A 1994 *Phys. Rev. B* **49** 1407

[15] Armitage N P, Fournier P, and Greene R L 2010 *Rev. Mod. Phys.* **82** 2421
[16] Greene R L, Mandal P R, Poniatowski N R, and Sarkar T 2020 *Annu. Rev. Condens. Matter Phys.* **11** 213
[17] Chu C W, Deng L Z, and Lv B 2015 *Physica C* **514** 290
[18] Weber C, Haule K, and Kotliar G 2010 *Nat. Phys.* **6** 574
[19] Pavarini E, Dasgupta I, Saha-Dasgupta T, Jepsen O, and Andersen O K 2001 *Phys. Rev. Lett.* **87** 047003
[20] de Mello E V L 2012 *Europhys. Lett.* **99** 37003
[21] Li H Z, Li H, Wang Z H *et al.* 2023 *npj Quantum Mater.* **8** 18
[22] Kohsaka Y, Azuma M, Yamada I *et al.* 2002 *J. Am. Chem. Soc.* **124** 12275
[23] Hanaguri T, Lupien C, Kohsaka Y *et al.* 2004 *Nature* **430** 1001
[24] Hanaguri T, Kohsaka Y, Davis J C *et al.* 2007 *Nat. Phys.* **3** 865
[25] Shen K M, Ronning F, Lu D H *et al.* 2005 *Science* **307** 901
[26] Hu C, Zhao J F, Gao Q *et al.* 2021 *Nat. Commun.* **12** 1356
[27] Hiroi Z, Kobayashi N, and Takano M 1994 *Nature* **371** 139
[28] Waku K, Katsufuji T, Kohsaka Y *et al.* 2004 *Phys. Rev. B* **70** 134501
[29] Ye C, Cai P, Yu R Z *et al.* 2013 *Nat. Commun.* **4** 1365
[30] Ronning F, Kim C, Feng D L *et al.* 1998 *Science* **282** 2067
[31] Hu C, Zhao J F, Ding Y *et al.* 2018 *Chin. Phys. Lett.* **35** 067403
[32] Pothuizen J J M, Eder R, Hien N T *et al.* 1997 *Phys. Rev. Lett.* **78** 717
[33] Kumagai Y, Oba F, Yamada I, Azuma M, and Tanaka I 2009 *Phys. Rev. B* **80** 085120
[34] He C P, Yu S L, Xiang T, and Li J X 2022 *Chin. Phys. Lett.* **39** 057401
[35] Leong W H, Yu S L, Xiang T, and Li J X 2014 *Phys. Rev. B* **90** 245102
[36] Song C L, Zhang H M, Zhong Y *et al.* 2016 *Phys. Rev. Lett.* **116** 157001
[37] Yuan Y H, Fan X M, Wang X T *et al.* 2021 *Nat. Commun.* **12** 2196
[38] Ren M Q, Yan Y J, Niu X H *et al.* 2017 *Sci. Adv.* **3** e1603238
[39] Gavioli L, Padovani M, Spiller E, Sancrotti M, and Betti M G 2003 *Appl. Surf. Sci.* **212** 47
[40] Ferbel L, Veronesi S, and Heun S 2003 *Appl. Surf. Sci.* **718** 122011
[41] Harima N, Matsuno J, Fujimori A *et al.* 2001 *Phys. Rev. B* **64** 220507
[42] Armitage N P, Ronning F, Lu D H *et al.* 2002 *Phys. Rev. Lett.* **88** 257001
[43] Taguchi M, Chainani A, Horiba K *et al.* 2005 *Phys. Rev. Lett.* **95** 177002
[44] Allen J W, Olson C G, Maple M B *et al.* 1990 *Phys. Rev. Lett.* **64** 595
[45] Ino A, Kim C, Nakamura M *et al.* 2000 *Phys. Rev. B* **62** 4137
[46] Li H W, Ye S S, Zhao J F, Jin C Q, and Wang Y Y 2021 *Sci. Bull.* **66** 1395
[47] Phillips P 2010 *Rev. Mod. Phys.* **82** 1719
[48] Wang Z Y and Shu D J 2021 *J. Phys. Chem. C* **125** 19259